TECHNICAL REPORT

Open Access

A LabVIEW software for Thellier paleointensity measurements with an automated three-component spinner magnetometer TSpin

Koji Fukuma[1*] and Masaru Kono[2]

Abstract

The Thellier method is classical but is still regarded as the most reliable method for paleointensity determination. Recently, many types of additional protocols have been advocated to ensure reliability and make laboratory work more laborious and time-consuming. An automated system coupling a magnetometer and an electric furnace is now of prime importance to cope with the increasing demand. Here, we describe a graphics-based program for controlling a fully automatic system combining a spinner magnetometer and a thermal demagnetizer, and for acquiring and processing the magnetization data. A single fluxgate sensor, which can measure the vector magnetization by spinning and translating a standard-sized 1-in. specimen, was calibrated with a rotatable reference specimen that can make the magnetization parallel or perpendicular to the spinning axis. By placing a cooling chamber between the furnace and the sensor for the updated system, the specimen can be heated up more efficiently to ensure an identical thermal history for the double heatings of the Thellier method. The direction of the vector magnetization was precisely obtained as well as the intensity, the results being comparable with those from an ordinary spinner magnetometer. We present an application of the fully automatic system for a Thellier measurement on a recent lava flow, which took about 24 h for approximately ten-step double heatings without manual operation.

Keywords: Paleointensity, Thellier method, Magnetometer

Background

With the increasing interest in past geomagnetic field intensities, much more reliable and abundant paleointensity determinations are required in recent years (e.g., Dunlop 2011). Published paleointensity data have been compiled in databases (Biggin et al. 2009; Brown et al. 2015) that allow users to find lack of reproducibility in the existing paleointensity results. Field tests for materials cooled in the known geomagnetic field revealed significant variations in obtained paleointensities within a single sampling site (e.g., Herrero-Bervera and Valet 2009; Yamamoto et al. 2015). Paleointensity experiments usually need to repeat double heatings at many temperature steps as in the Thellier method (Thellier and Thellier 1959). This experimental procedure is intrinsically laborious and time-consuming. Even if a preliminary sample selection is applied, many samples cannot meet the criteria for acceptable paleointensity data, and the criteria are becoming increasingly more rigorous (e.g., Paterson et al. 2014). Chemical or magnetic domain alteration during heating and/or multidomain effects hamper the determination of paleointensities (e.g., Valet et al. 1996). To evaluate paleointensity data, a variety of additional procedures such as the partial thermoremanent magnetization (pTRM) check (Coe 1967), pTRM tail check (Riisager and Riisager 2001), or the IZZI protocol (Yu and Tauxe 2005) have been introduced, but they require more time and labor.

Although paleomagnetic measurements have been mostly performed with a manual combination of a

*Correspondence: kfukuma@mail.doshisha.ac.jp
[1] Department of Environmental System Science, Doshisha University, Kyotanabe 610–0394, Japan
Full list of author information is available at the end of the article

thermal or alternating field (AF) demagnetizer and a remanence magnetometer, several automated magnetometers have been developed. In the early 1980s, AF demagnetizers were incorporated into fully automated spinner magnetometer systems (Kono et al. 1981) and later coupled with superconducting magnetometers (Kirschvink et al. 2008). Then a commercially available 2G system, arranged with a superconducting magnetometer and an AF demagnetizer in series on a horizontal sample track, enabled AF demagnetization and measurement of long cores or discrete specimens automatically. The 2G automatic systems are now widely used for retrieving paleomagnetic directions in many laboratories worldwide. Recently, some updated systems with AF demagnetizers based on the 2G superconducting magnetometer were also developed (e.g., Morris et al. 2009; Wack and Gilder 2012).

An automatic system such as the 2G system is not widely used for paleointensity studies. This is because housing a thermal demagnetizer with a superconducting or spinner magnetometer is a challenge. To date, automated systems based on a vibrating sample magnetometer (VSM) have been developed for paleointensity measurements in Borok, Russia (e.g., Shcherbakova et al. 2008), and Paris (Le Goff and Gallet 2004). The system developed in Borok was commercially distributed as an Orion VSM and used after some modification in other laboratories (Dunlop 2008; Poidras et al. 2009). Muxworthy (2010) attempted the Wilson method (Wilson 1962) using the Orion VSM, which is capable of measuring three components of magnetization at elevated temperatures. The Triaxe VSM in Paris provided a large amount of paleointensity data on archeological materials with a Wilson-type method (Gallet and Le Goff 2006; Gallet et al. 2009). Thellier experiments can also be performed by the automated VSMs using small-sized $1\,cm^3$ cubes or minicores. Precisely orienting such a small specimen is difficult, and therefore, a standard 1-in. cylinder is separately prepared for directional studies (e.g., Shcherbakova et al. 2014). High-temperature experiments using a superconducting magnetometer were attempted but not operated in a fully automatic mode for routine measurements (Sugiura 1989; Tanaka et al. 1995).

In an ordinary spinner magnetometer with a fluxgate sensor, a specimen is rotated about a single axis, and the orientation needs to be manually changed for measuring the three components of magnetization. Although automatic measurement might seem difficult to perform along with demagnetization, Kono et al. (1981) made it possible to combine an AF demagnetizer and a spinner magnetometer by using a tumbler. For thermal demagnetization or paleointensity measurements, Kono et al. (1991) developed an automated three-component

magnetometer with a thermal demagnetizer called TSpin. In this system, a standard-sized paleomagnetic specimen is translated along the spinning axis; therefore, the axial magnetization can be measured as well as the in-plane components perpendicular to the spinning axis. The specimen is further translated into an electric furnace for thermal demagnetization and pTRM acquisition.

To the best of our knowledge, no automated spinner magnetometer is available other than TSpin, with which Thellier paleointensity experiments can be performed on a routine basis. Hotspin 2, developed by Wack and Matzka (2007), can measure the full vector of remanence using six fluxgate sensors as a specimen is heated up to 350 °C by flowing hot air. The maximum temperature is not enough to fully demagnetize specimens containing magnetite or Ti-poor titanomagnetite. In addition, a coil imparting thermoremanent magnetization is not incorporated; therefore, paleointensity experiments cannot be performed with Hotspin 2.

Here, we report a newly developed LabVIEW software to control TSpin for Thellier paleointensity experiments, to analyze the data, and then to generate Zijderveld, Arai, and Roquet diagrams. Some minor modifications of the hardware are also described. The graphics-based software makes setting and monitoring of the automated system easier, helps minimize human-induced errors, and is flexibly adaptable to complicated procedures. Calibration using a standard specimen and test measurements on some volcanic materials is also reported.

Hardware

The design of TSpin is essentially the same as that of the original system (Kono et al. 1991), but the two systems were constructed for routine measurements. A fluxgate sensor and an electric furnace for thermal demagnetization are the principal components of TSpin (Fig. 1). A standard 1-in. cylindrical specimen is translated between the sensing region and the electric furnace. Unlike the original system, a cooling chamber equipped with a blower is built between the furnace and the sensing region. These three components are housed in a three-layer μ-metal magnetic shield. A long solenoid coil,
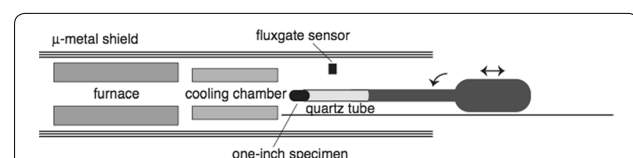

Fig. 1 A schematic illustration of an automated three-component spinner magnetometer with a thermal demagnetizer TSpin. A fluxgate sensor is set to measure the radial component of the magnetic field for a spinning and translating specimen

covering the furnace and the cooling chamber, produces a uniform magnetic field to impart pTRM. The residual magnetic field in the cooling chamber is kept less than 10 nT by applying a backfield using the solenoid coil after each Thellier measurement. When the heating process is finished, the specimen is translated from the furnace to the cooling chamber within approximately 1 s, because of which cooling during the translation is expected to be negligible. This heating–cooling process is not essentially different from the procedure using a mobile furnace (Kissel and Laj 2004).

A 1-in. cylindrical specimen, which is fixed to the quartz glass tube holder by using quartz fiber, can be heated up to a maximum of 700 °C. The cylindrical axis of the specimen is set parallel to that of the glass tube, which is also fixed along the spinning axis by using a collet. Thus, the cylindrical specimen's axis aligns parallel to the spinning axis of TSpin. After adjusting the angle of the glass tube so as to make the specimen's orientation marker line vertical using a laser level (Fig. 2), the collet is tightened to fix the specimen to the spinning axis. The specimen's marker can be adjusted within a few degrees from the vertical. Fixing the glass tube with the collet reduces wobbling during spinning and enables precise orientation of the specimen.

Thirty-two slits on a rotating disk fixed to the spinning axis are used to monitor the spinning angle with a photo-interrupter, and one of the slits is marked as the zero angle, which is used to orient the specimen's marker line. Heating and cooling positions are identified with another photo-interrupter according to the translation. When measuring the magnetization, spinning is repeated at ten or more axial positions that are adjusted with 1-mm-spaced slits and a photo-interrupter. A specimen is translated over a 15-cm interval parallel to the axis near the fluxgate sensor.
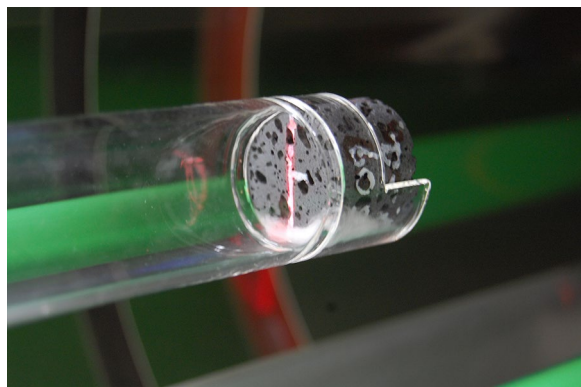

Fig. 2 A standard-sized cylindrical specimen mounted on a glass tube holder with glass fiber. An orientation marker line is set vertical using a *red* laser line

A single fluxgate sensor is fixed approximately 5 cm away from the spinning axis to measure the radial component of the magnetic field produced by a specimen. Translation of the specimen along the axis allows both the axial and in-plane components of magnetization to produce signals for the radial fluxgate sensor, by decomposition of the signal as described by Kono et al. (1991). Amplification of the output voltage from the fluxgate sensor can be selected from 1×, 10×, 100×, and 1000×, depending on a specimen's magnetization intensity.

The electric furnace of TSpin, operated by a thermocontroller CHINO KP1000, performs thermal demagnetization and pTRM acquisition depending on whether the solenoid coil is turned on or off. To replicate the same thermal history for demagnetization and pTRM acquisition, the furnace was heated up to a target temperature before inserting a specimen. The reason for this is that ramping up the temperature after inserting a specimen sometimes induces temperature overshoot and results in different temperature histories for zero- and in-field steps. The temperature was calibrated by using a dummy specimen where two K-type thermocouples are plastered with cement at the center and on the surface. While heating a specimen in the furnace, the temperature is monitored by an R-type thermocouple placed approximately 1 cm below a specimen. The cooling chamber is placed at the center of the magnetic shield case, ensuring a minimum residual field during demagnetization.

Software

A LabVIEW software controls spinning and translating the specimen, sets the furnace temperature through the thermocontroller, controls a direct current source for the solenoid coil, and obtains the signal from the fluxgate sensor. A digital input/output board CONTEC PIO 32/32F(PCI), installed in a PCI bus of a personal computer, sends on/off signals to the spinning and translating motors, the solenoid coil, and a blower, whereas it receives signals from the photo-interrupters monitoring the position and angle of a specimen. The thermocontroller is operated through an RS232C port, and the current source is connected to a USB port. An analog input board, INTERFACE PCI-3135, picks up the output voltage in the range of ±10 V from the fluxgate sensor and converts it into a 16-bit digital signal. Driver softwares that enable LabVIEW to communicate with the digital or analog boards are available from the respective manufacturer.

Before starting a Thellier measurement, users need to specify the temperature steps, pTRM check and pTRM tail check steps in the LabVIEW controlling software, as well as the applied field for pTRM acquisition (Fig. 3). The software allows users to select a temperature
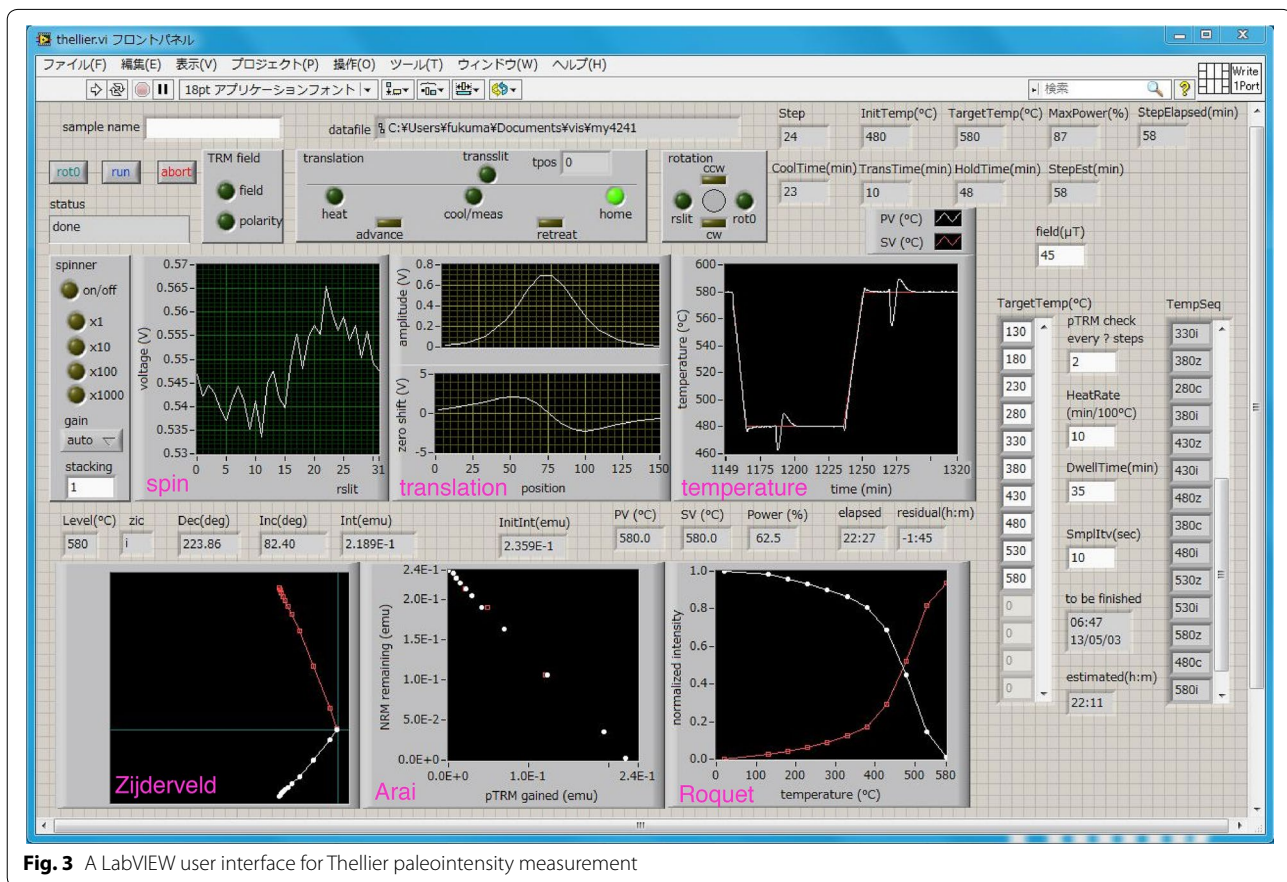
Fig. 3 A LabVIEW user interface for Thellier paleointensity measurement

sequence from a menu of customized sequences or to specify it by editing a text file. After users select whether to assign additional steps of the pTRM check or tail check or not, the software generates a sequence of zero- or in-field treatments for the Thellier experiment. This automatic sequence generation helps prevent human-induced errors. At present, the Coe version of the Thellier method is assumed, but any other version such as the IZZI protocol (Yu and Tauxe 2005) can be introduced with minor modifications. A heating rate of 10 °C/min and a hold time in the furnace of about 30 min are typically specified, but these parameters are adjustable depending on the measured specimen. Users can choose a relatively high heating rate because a specimen is out of the furnace when the furnace temperature is changed. After heating up the empty furnace, a specimen is inserted into the furnace that has already reached the temperature of the next step.

When a specimen is cooled down after demagnetization or pTRM acquisition, it is brought back to the sensor region. Prior to measuring the remanence, the gain of the fluxgate sensor is adjusted by scanning the output voltage at several positions as it is pulled out of the cooling

chamber. If the output voltage exceeds the acceptable range ±10 V of the analog board, the gain is switched to the lower one. When pushing back the specimen, measurements are taken by spinning the specimen at 15 different positions spanning approximately 15 cm near the fluxgate sensor. The fluxgate output signal represents the radial component of the magnetic field that is generated by both the in-plane and axial components of the specimen magnetization. The output voltage was acquired 32 times for a single rotation in response to the rotating slits. A quasi-sinusoidal response curve is drawn for each rotation as shown in the upper half of Fig. 3.

The fast Fourier transform (FFT) is applied to spinning data for each of the 15 positions, by which the amplitude, zero shift, and phase are derived as a function of the axial position. Assuming that the dipole term of the specimen's magnetization dominates the output signal, the magnetization is given by the magnitude of the in-plane component m_h, its angle ϕ, and the magnitude of the axial component m_z in a cylindrical coordinate frame (Kono et al. 1991). ϕ should be independent of the axial position and therefore is calculated by the weighted average of the phase angles of each set of spinning

data. On the other hand, the amplitude and zero shift vary with the specimen position and can be related to $m_h \cdot \sin^3 \theta \cdot (3 \sin^2 \theta - 1)$ and $m_z \cdot \sin^3 \theta \cdot 3 \sin \theta \cos \theta$, respectively. $\theta = \tan^{-1}(s/z)$ is specified by the specimen's axial position z and the sensor displacement from the axis s. The ratio of the power of these dipole components with respect to the total power is larger than 0.999 in most cases, indicating that the higher harmonics are negligibly small compared to the dipole signal.

Now that the three components of magnetization (m_h, ϕ, m_z) in a cylindrical coordinate frame have been determined for each step of a Thellier measurement, real-time visualization in Zijderveld, Arai, and Roquet diagrams is realized before completing the scheduled sequence (Fig. 3; lower half of the window). These diagrams help users check the ongoing behavior and decide whether to interrupt the sequence when problems arise. Typically, a single Thellier experiment using TSpin takes approximately 24 h to complete a suite of double heatings at about ten temperature steps, including pTRM checks. If users encounter problems and halt an automated measurement, much more machine time is saved. Indeed, in most cases, the Thellier measurement by TSpin automatically continues unattended overnight, and no additional operation is needed except for the initial settings.

For each spinning, the software stores the raw voltage data from the fluxgate sensor. These raw data make it possible to recalculate the magnetization parameters if the calibration constant is revised later. The target and measured temperatures of the furnace are displayed on the screen (Fig. 3) and stored to examine the status of heating and cooling. The processed data for drawing real-time Zijderveld, Arai, and Roquet diagrams are saved in individual files that are used subsequently for the same types of drawing. Besides the main software for the Thellier experiments, independent softwares are prepared for room-temperature measurements, which is useful for calibration measurements, and for steering the digital board when problems are encountered.

Calibration

We prepared a standard specimen by fixing a tiny needle-like magnet in synthetic resin. This standard specimen is specially designed to be rotatable so as to set the magnetization direction perpendicular or parallel to the spinning axis (Fig. 4). Therefore, both the in-plane and axial components of magnetization can be calibrated with a single standard specimen. The magnetic moment of the specimen was measured with an ordinary spinner magnetometer (Natsuhara Giken, ASpin) at Doshisha University, and the measured value of 9.996×10^{-5} Am^2 is taken as the reference value. This means that our calibration is not absolute; rather, it should be regarded as a relative
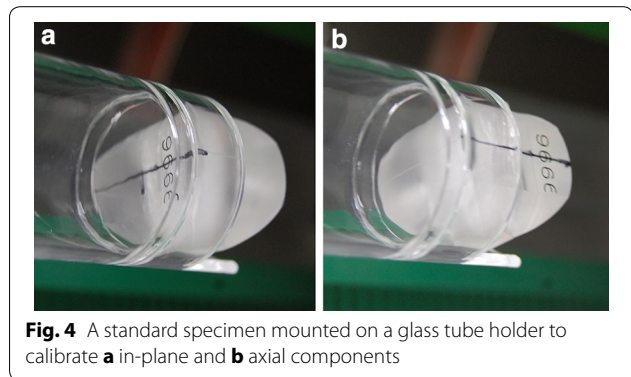

Fig. 4 A standard specimen mounted on a glass tube holder to calibrate **a** in-plane and **b** axial components

inter-calibration with the ordinary spinner magnetometer. However, the reference value is reliable because the ordinary spinner magnetometer is routinely cross-calibrated using several calibration specimens.

Making the standard specimen's magnetization parallel or perpendicular to the spinning axis, we can calibrate the axial or in-plane components, respectively. Measurements were repeated by rotating the specimen 180° in order to cancel out undesirable voltage offsets. When measuring the axial component, the specimen is translated against the fluxgate sensor. The output voltage should vary as a function of the position along the spinning axis (Kono et al. 1991). Least square fitting based on the dipole curve can provide m_z expressed in V that is related to the magnetic moment of the standard specimen in Am^2. For the in-plane component, the moment direction is precisely assigned to be vertical using a laser level (Fig. 3), and then, spinning was repeated at several different positions. The amplitude of the output voltage is calculated by applying FFT to each set of spinning data, and the relationship between the voltage amplitude and the axial position gives m_h, which is related to the reference magnetic moment.

Calibration factors for both the axial and in-plane components were determined for each amplification gain. At the lowest gain 1×, the calibration factor is approximately 1.6×10^{-4} Am^2/V. This value determines the upper limit of the measured magnetic moment as 1.6×10^{-3} Am^2, considering the input limit of the analog board ± 10 V. Although the standard specimen has a relatively high magnetic moment of 9.996×10^{-5} Am^2, we could directly calibrate up to the 100× range. If we extend the range up to 1000× and assume a voltage resolution of 0.05 V, the sensitivity of TSpin turns out to be approximately 1×10^{-8} Am^2.

The phase angle of the in-plane component is also necessary to be calibrated for the constitution of the mutually independent three components in a cylindrical coordinate system. If the specimen is rotated step by

step and one of 32 rotating slits is detected by an optical interruptor, the output voltage is precisely determined as a function of the phase angle. Because the specimen is actually rotated at a constant angular speed, however, a significant difference between the phase of the output signal and the detected phase angle emerges. The phase angle derived by FFT analysis of the output signal and that given by the slit reading are compared, after which the phase lag is determined and used as the phase angle adjustment for the in-plane component. In routine measurements, the spinning angular speed and the sense of spin remain unchanged for the calibration measurement.
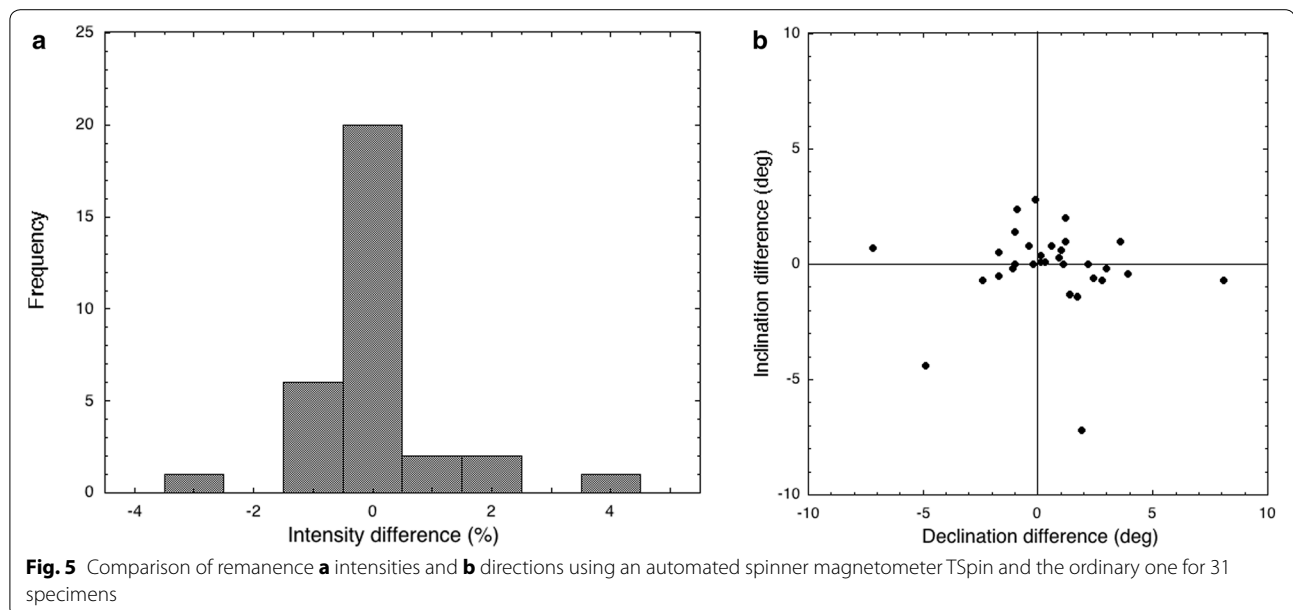
We compared the remanent magnetizations measured by TSpin and the ordinary spinner magnetometer ASpin. These two spinner magnetometers were inter-calibrated with each other using a standard specimen. Thirty-one standard-sized cylindrical specimens were prepared from a recent basaltic lava flow that erupted in Miyakejima, Japan. The averages of the remanence intensities, measured by TSpin and ASpin, were exactly 2.22×10^{-4} Am^2 correct to the three significant digits. To compare the intensities of individual specimens, we observed that the differences from the average intensity concentrate around zero and the standard deviation was only 1.09 % (Fig. 5a). Further, the remanence directions do not significantly differ on the individual specimen level. The standard deviation of the declination, 2.74°, is larger than that of the inclination, 1.81°, as shown by the laterally distributed directions in Fig. 5b. These remanence directions are shown in a specimen coordinate frame; therefore, the declination values are directly influenced by the accuracy of orienting the marker lines with a laser level, but the
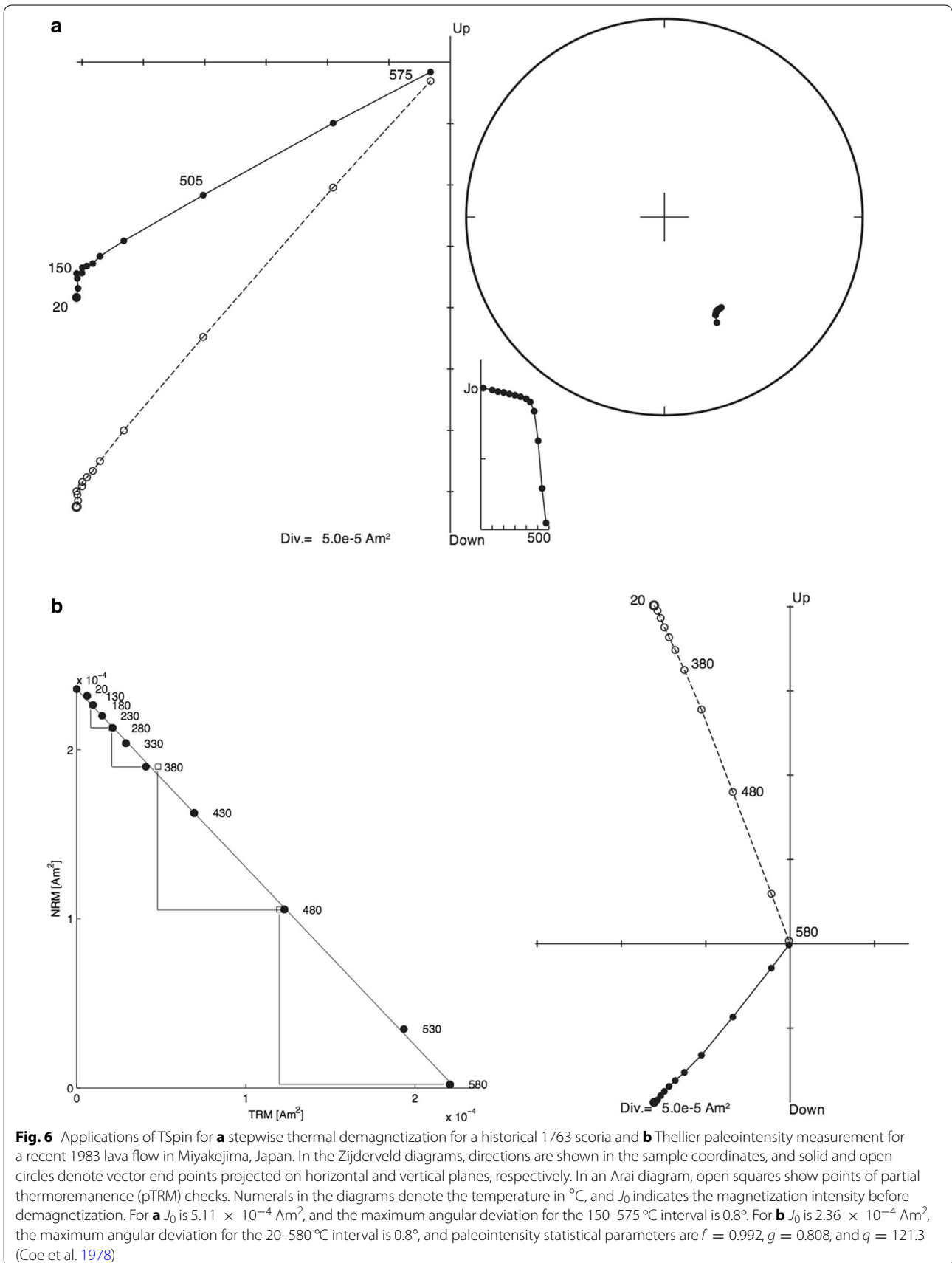
inclination values are determined only by the ratio of the in-plane and axial components measured with a single fluxgate sensor.

Applications

To demonstrate the advantages of the automated measurement by TSpin, first we present a test measurement accompanied by stepwise thermal demagnetization on a historic scoria from the 1763 eruption in Miyakejima (Fig. 6a). This specimen exhibits a narrow unblocking temperature range concentrated around 500 °C. The high-temperature magnetization component is prominent and extremely stable during the thermal demagnetization as indicated by the small maximum angular deviation of 0.8° for the segment 150–575 °C (Kirschvink 1980). In addition to the stable component, we can observe a minor magnetization component below 150 °C. The minor component, which was probably acquired during laboratory storage, is clearly distinguishable owing to the sharp bend between the two straight lines on the Zijderveld diagram. However, this is unexpected for manually measured specimens. For TSpin, it is not necessary to remove and attach a specimen to a sample holder at each demagnetization step; therefore, orientation errors between neighboring demagnetization steps are avoidable. Moreover, because a specimen stays inside a single magnetic shield case during the course of repeated measurements and thermal demagnetizations, spurious magnetization is hardly acquired, unlike when the specimen is manually handled outside the shield case.

A Thellier paleointensity result obtained by TSpin is shown for a specimen collected from the 1983 lava flow

Fig. 5 Comparison of remanence **a** intensities and **b** directions using an automated spinner magnetometer TSpin and the ordinary one for 31 specimens

Fig. 6 Applications of TSpin for **a** stepwise thermal demagnetization for a historical 1763 scoria and **b** Thellier paleointensity measurement for a recent 1983 lava flow in Miyakejima, Japan. In the Zijderveld diagrams, directions are shown in the sample coordinates, and solid and open circles denote vector end points projected on horizontal and vertical planes, respectively. In an Arai diagram, open squares show points of partial thermoremanence (pTRM) checks. Numerals in the diagrams denote the temperature in °C, and J_0 indicates the magnetization intensity before demagnetization. For **a** J_0 is 5.11 × 10^{-4} Am^2, and the maximum angular deviation for the 150–575 °C interval is 0.8°. For **b** J_0 is 2.36 × 10^{-4} Am^2, the maximum angular deviation for the 20–580 °C interval is 0.8°, and paleointensity statistical parameters are $f = 0.992$, $g = 0.808$, and $q = 121.3$ (Coe et al. 1978)

in Miyakejima as a typical example (Fig. 6b). We applied the Coe version of the Thellier method to specimens of recent or historical lavas and scorias from Miyakejima using the two TSpin systems. An extremely well-defined straight line covering the entire temperature range up to 580 °C is visible on the Arai diagram (Fig. 6b). The resultant paleointensity of $47.4 \pm 0.3 \, \mu T$, determined from the entire measured temperature range 20–580 °C, does not greatly deviate from the expected value of $45.1 \, \mu T$ that is calculated for the sampling site from the International Geomagnetic Reference Field model. On the Zijderveld diagram, the magnetization decays along straight lines on the projections for both horizontal and vertical planes. As demonstrated for the stepwise thermal demagnetization (Fig. 6a), we did minimize the chances for orientation error and acquisition of spurious magnetization by avoiding manual handling of the specimen. Furthermore, the specimen is inserted into the preheated furnace, which ensures identical thermal histories both for zero- and in-field steps of the same temperature.

Concluding remarks

An automated three-component spinner magnetometer equipped with a thermal demagnetizer TSpin is utilized for routine operations for Thellier paleointensity experiments with a LabVIEW controlling software. TSpin has several advantages over conventional manual measurements. First, a Thellier measurement that is very laborious and time-consuming can be performed overnight without any user intervention. This enables a larger number of Thellier measurements to be made, in which uninterpretable results are often obtained. Second, the chance of an orientation error or acquisition of spurious magnetization is almost completely eliminated, because a series of remanence measurements combined with thermal demagnetization or pTRM acquisition continues in a magnetic shield case without manual handling of a specimen. Thus, TSpin helps us to clearly define linear segments on Zijderveld or Arai diagrams. Because TSpin can accommodate a standard-sized cylindrical specimen, remanence directions can also be reliably measured as the intensities. A collet and a laser level for fixing a glass tube holder help decrease declination or inclination errors significantly. Automated measurements by TSpin are arranged at the start using the LabVIEW software, which controls all the components of TSpin, monitors the temperature, acquires and analyzes magnetometer data, and enables real-time visualization for the entire measurement sequence. The software can be flexibly modified so as to incorporate any other protocols, such as determining temperature steps automatically or repeating rotation and translation to measure weakly magnetized specimens.

Author details
[1] Department of Environmental System Science, Doshisha University, Kyotanabe 610–0394, Japan. [2] Tokyo Institute of Technology, Nakano-ku, Tokyo 164-0013, Japan.

References
Biggin AJ, Strik GHMA, Langereis CG (2009) The intensity of the geomagnetic field in the late-Archaean: new measurements and an analysis of the updated IAGA palaeointensity database. Earth Planets Space 61:9–22. doi:10.1186/BF03352881

Brown MC, Donadini F, Korte M, Nilsson A, Korhonen K, Lodge A, Lengyel SN, Constable CG (2015) GEOMAGIA50.v3: 1. General structure and modifications to the archeological and volcanic database. Earth Planets Space. doi:10.1186/s40623-015-0232-0

Coe RS (1967) Paleointensities of the Earth's magnetic field determined from Tertiary and Quaternary rocks. J Geophys Res 72:3247–3262. doi:10.1029/JZ072i012p03247

Coe RS, Gromme S, Mankinen EA (1978) Geomagnetic paleointensities from radiocarbon-dated lava flows on Hawaii and the question of the Pacific nondipole low. J Geophys Res 83:1740–1756. doi:10.1029/JB083iB04p01740

Dunlop DJ (2008) Paleointensity determination using continuous thermal measurements by a high-temperature vibrating thermomagnetometer. Geochem Geophys Geosys. doi:10.1029/2008GC002054

Dunlop DJ (2011) Physical basis of the Thellier–Thellier and related paleointensity methods. Phys Earth Planet Int 187:118–138. doi:10.1016/j.pepi.2011.03.006

Gallet Y, Le Goff M (2006) High-temperature archeointensity measurements from Mesopotamia. Earth Planet Sci Lett 241:159–173. doi:10.1016/j.epsl.2005.09.058

Gallet Y, Hulot G, Chulliat A, Genevey A (2009) Geomagnetic field hemispheric asymmetry and archeomagnetic jerks. Earth Planet Sci Lett 284:179–186. doi:10.1016/j.epsl.2009.04.028

Herrero-Bervera E, Valet J-P (2009) Testing determinations of absolute paleointensity from the 1955 and 1960 Hawaiian flows. Earth Planet Sci Lett 287:420–433. doi:10.1016/j.epsl.2009.08.035

Kirschvink JL (1980) The least-squares line and plane and the analysis of paleomagnetic data. Geophys J R Astr Soc 62:699–718. doi:10.1111/j.1365-246X.1980.tb02601.x

Kirschvink JL, Kopp RE, Raub TD, Baumgartner CT, Holt JW (2008) Rapid, precise, and high-sensitivity acquisition of paleomagnetic and rock-magnetic data: development of a low-noise automatic sample changing system for superconducting rock magnetometers. Geochem Geophys Geosys. doi:10.1029/2007GC001856

Kissel C, Laj C (2004) Improvements in procedure and paleointensity selection criteria (PICRIT-03) for Thellier and Thellier determinations: application to Hawaiian basaltic long cores. Phys Earth Planet Int 147:155–169. doi:10.1016/j.pepi.2004.06.010

Kono M, Hamano Y, Nishitani T, Tosha T (1981) A new spinner magnetometer: principles and techniques. Geophys J R Astr Soc 67:217–227. doi:10.1111/j.1365-246X.1981.tb02744.x

Kono M, Hoshi M, Yamaguchi K, Nishi Y (1991) An automatic spinner magnetometer with thermal demagnetization equipment. J Geomag Geoelectr 43:429–443. doi:10.5636/jgg.43.429

Le Goff M, Gallet Y (2004) A new three-axis vibrating sample magnetometer for continuous high-temperature magnetization measurements: applications to paleo- and archeo-intensity determinations. Earth Planet Sci Lett 229:31–43. doi:10.1016/j.epsl.2004.10.025

Morris ER, Schillinger W, Coe RS, Pluhar CJ, Jarboe NA (2009) Automating the 2G superconducting rock magnetometer for single-solenoid alternating field demagnetization. Geochem Geophys Geosys. doi:10.1029/2008GC002289

Muxworthy AR (2010) Revisiting a domain-state independent method of palaeointensity determination. Phys Earth Planet Int 179:21–31. doi:10.1016/j.pepi.2010.01.003

Paterson GA, Tauxe L, Biggin AJ, Shaar R, Jonestrask LC (2014) On improving the selection of Thellier-type paleointensity data. Geochem Geophys Geosys. doi:10.1002/2013GC005135

Poidras T, Camps P, Nicol P (2009) Controlled atmosphere vibrating thermomagnetometer (CatVTM): a new device to optimize the absolute paleointensity determinations. Earth Planets Space 61:101–110. doi:10.1186/BF03352889

Riisager P, Riisager J (2001) Detecting multidomain magnetic grains in Thellier palaeointensity experiments. Phys Earth Planet Int 125:111–117. doi:10.1016/S0031-9201(01)00236-9

Shcherbakova VV, Lubnina NV, Shcherbakov VP, Mertanen S, Zhidkov GV, Vasilieva TI, Tsel'movich VA (2008) Palaeointensity and palaeodirectional studies of early Riphaean dyke complexes in the Lake Ladoga region (Northwestern Russia). Geophys J Int 175:433–448. doi:10.1111/j.1365-246X.2008.03859.x

Shcherbakova VV, Shcherbakov VP, Zhidkov GV, Lubnina NV (2014) Palaeointensity determinations on rocks from Palaeoproterozoic dykes from the Kaapvaal Craton (South Africa). Geophys J Int 197:1371–1381. doi:10.1111/j.1365-246X.2008.03859.x

Sugiura N (1989) Measurement of magnetization at high temperatures and the origin of thermoremanent magnetization a review. J Geomag Geoelectr 41:3–17. doi:10.5636/jgg.41.3

Tanaka H, Athanassopoulos JDE, Dunn JR, Fuller M (1995) Paleointensity determinations with measurements at high temperature. J Geomag Geoelectr 47:103–113. doi:10.5636/jgg.47.103

Thellier E, Thellier O (1959) Sur l'intensité du champ magnétique terrestre dans le passé historique et géologique. Ann Geophys 15:285–376

Valet J-P, Brassart J, Le Meur I, Soler V, Quidelleur X, Tric E, Gillot P-Y (1996) Absolute paleointensity and magnetomineralogical changes. J Geophys Res 101:25029–25044. doi:10.1029/96JB02115

Wack M, Matzka J (2007) A new type of a three-component spinner magnetometer to measure the remanence of rocks at elevated temperature. Earth Planets Space 59:853–862. doi:10.1186/BF03352747

Wack MR, Gilder SA (2012) The SushiBar: an automated system for paleomagnetic investigations. Geochem Geophys Geosys. doi:10.1029/2011gc003985

Wilson RL (1962) An instrument for measuring vector magnetization at high temperatures. Geophys J R Astr Soc 7:125–130. doi:10.1111/j.1365-246X.1962.tb02257.x

Yamamoto Y, Torii M, Natsuhara N (2015) Archeointensity study on baked clay samples taken from the reconstructed ancient kiln: implication for validity of the Tsunakawa-Shaw paleointensity method. Earth Planets Space. doi:10.1186/s40623-015-0229-8

Yu Y, Tauxe L (2005) Testing the IZZI protocol of geomagnetic field intensity determination. Geochem Geophys Geosyst. doi:10.1029/2004GC000840